Defence Technology 15 (2019) 254–263

Contents lists available at ScienceDirect

Defence Technology

journal homepage: www.elsevier.com/locate/dt

Special materials in pyrotechnics VII: Pyrotechnics used in thermal batteries☆

Ernst-Christian Koch

Lutradyn Energetic Materials Science & Technology, 67661, Kaiserslautern, Germany

ARTICLE INFO

Article history:
Received 2 January 2019
Received in revised form
28 January 2019
Accepted 26 February 2019
Available online 1 March 2019

Keywords:
Barium chromate
Heat-powder
Iron
Lithium
Molten salt
Potassium perchlorate
Pyrotechnics
Thermal battery
Zirconium

ABSTRACT

Thermal batteries are unique direct current (DC) electrical power sources with long shelf live, high reliability and higher power density than classical alkaline batteries. This paper gives a brief overview into the working principle of thermal batteries and reviews the properties of zirconium/barium chromate (Zr/$BaCrO_4$) pyrolant previously used as first fire and iron/potassium perchlorate (Fe/$KClO_4$) pyrolant (Heat), commonly applied as heating pellet in thermal batteries and its hazard properties. The review gives 64 references to the public domain. CAS-Nos. Zr: [7440-67-7], $BaCrO_4$: [10294-40-3], Fe: [7439-89-6], $KClO_4$: [7778-74-7], Viton: [9011-17-0].

CAS-Nos. Zr: [7440-67-7], $BaCrO_4$: [10294-40-3], Fe: [7439-89-6], $KClO_4$: [7778-74-7], Viton: [9011-17-0].

1. Introduction and general design of thermal batteries

Thermal batteries, also known as thermally activated batteries, thermal reserve batteries or molten salt batteries work in a similar way as regular alkaline batteries however, they contain a solid ionic as an electrolyte which does not conduct electricity at ambient temperature and hence the battery does not undergo any kind of deterioration and can have shelf lives in excess of 25 years. To become activated these batteries require heat input to liquefy the electrolyte and become electrically conductive. Due to the very high electrical conductivity of molten salts thermal batteries provide higher power densities than classical batteries. Fig. 1 compares a thermal battery cell (Li_xSi_y/FeS_2) with ambient temperature battery systems Zn/AgO and Li/CF. Both long shelf life and high-power density make thermal batteries ideal choice for ordnance systems such as missiles and guided munitions, however they are also high price items with limited energy density.

Fig. 2 schematically depicts a typical thermal battery and its components [3]. The cell assembly comprises an anode, the separator with the immobilized electrolyte mixture, the cathode and a pyrotechnic heating pellet. Depending on the cell voltage the battery typically contains a stack of several cells. While older battery designs comprise an external lateral pyrotechnic ignition (fuse strip) triggered by an electric match nowadays more commonly an electrical igniter fires down the central cavity of the cell stack to ignite the pyrotechnic pellets [4]. This assembly is rigidly wrapped in multiple layers of thermal insulation and firmly encased in an airtight stainless-steel cylinder which bears glass-sealed electrical output terminals and terminals for the electrical igniter.

1.1. Anode material

Lithium is the element of choice for the anode in electrochemical applications due to its superior electrochemical potential ($Li/Li^{+\cdot}$- 3.04V) and its high specific Coulombic capacity, due to its low atomic weight and low density ($\rho = 0.534\,g\,cm^{-3}$). However, for practical reasons - as pure lithium has too low a melting point (mp: 180 °C) - compounds such as, LiAl (mp: 700 °C), $Li_{13}Si_4$ (mp: 722 °C), Li_7Si_3 (mp: 752 °C) are used as anode materialism also Li-

---

☆ Though part VI Ref. [1] has appeared in 2007 Part V Ref. [2] was not published until 2008.

E-mail address: e-c.koch@lutradyn.com.
URL: http://www.lutradyn.com

Peer review under responsibility of China Ordnance Society.

https://doi.org/10.1016/j.dt.2019.02.004

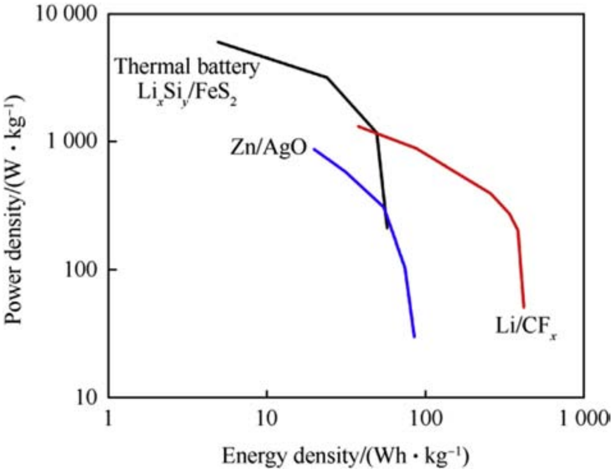

Fig. 1. Comparison of power and energy density of thermal battery cell with common ambient temperature cells.

rich borides also been explored as alternatives to both LiAl and $Li_{13}Si_4$ [6,7]. Another common anode material is calcium which has a lower electrochemical potential than lithium but which also bears a higher melting point (mp: 845 °C). Typical anodes in batteries are not made from pure lithium but comprise about 2/3 of high melting lithium alloy, immobilized with 2/9 sponge iron powder and 1/9 electrolyte premix, the latter containing up to 35 wt% MgO as porous binder.

1.2. Cathode

Typical cathode material in thermally activated batteries is iron(II) sulfide (FeS_2) bearing the S_2^{2-} anion. A general advantage of FeS_2 is its insolubility in molten alkali halide eutectics. Therefore it cannot diffuse to the anode and cause short circuiting [8].

On the flipside, FeS_2 decomposes at temperatures around 450 °C according to Eq. (1) [9,10].

$$FeS_2 \xrightarrow{\qquad\qquad} FeS_{1.14} + 0.43S_2 \tag{1}$$

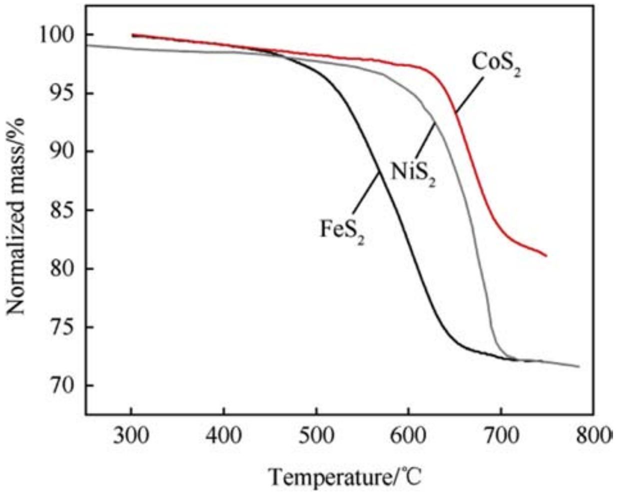

Fig. 3. Thermal decomposition of FeS_2 NiS_2 and CoS_2 after Ref. [12].

and is a semiconductor in this temperature regime. Hence, cobalt(II) sulfide (CoS_2) is used to a greater extent in recent years in thermal batteries [11]. Though CoS_2 is more expensive than FeS_2 it has a favourably higher decomposition temperature of ~650 °C (see Fig. 3) and exhibits near metal type conductivity at elevated temperatures [12] (Table 1).

The reactions upon discharge can be summarized by the following Eqs. (2)–(5). In case of cobalt(II) disulfide as the cathode material a similar sequence is understood to occur [10].

$$FeS_2 + \frac{3}{2}Li^+ + \frac{3}{2}e^- \rightarrow \frac{1}{2}Li_3Fe_2S_4(\}Z - \text{phase}\}) \tag{2}$$

$$(1\text{-}x)\ Li_3Fe_2S_4 + (1\text{-}2x)\ Li^+ + (1\text{-}2x)\ e\text{-} \longrightarrow Li_{2\text{-}x}Fe_{1\text{-}x}S_2 + Fe_{1\text{-}x}S + (1\text{-}x)\ S_2 \tag{3}$$

$$Li_{2\text{-}x}Fe_{1\text{-}x}S_2 \longrightarrow Li_2FeS_2\ (\text{“X-phase”}) \tag{4}$$

$$Li_2FeS_2 + 2e^- \longrightarrow Li_2S + Fe + S^{2-} \tag{5}$$

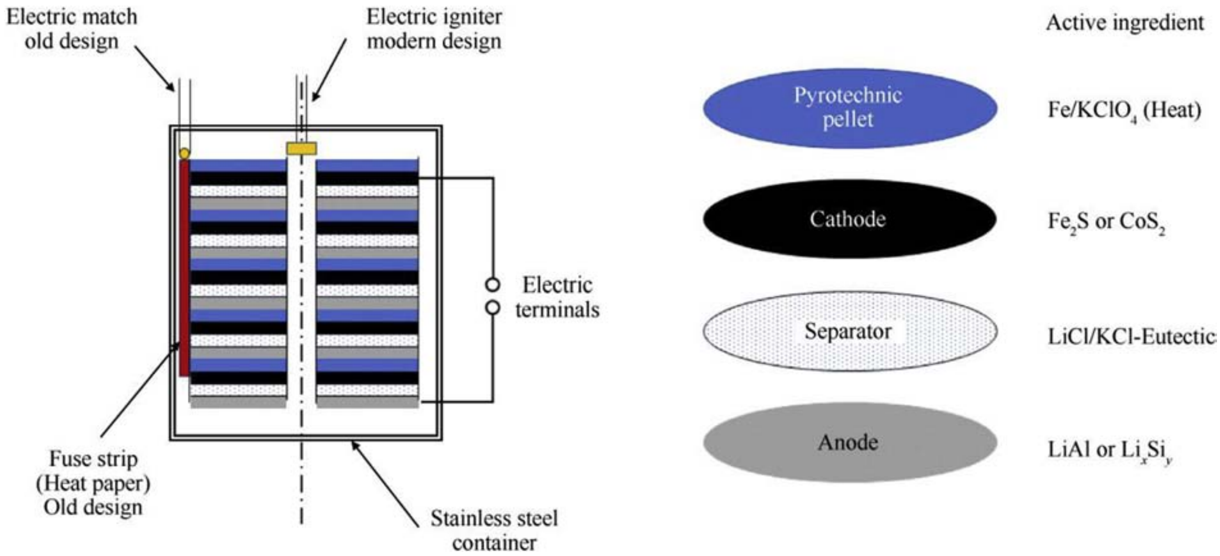

Fig. 2. Schematic Cut-away drawing of a thermal battery after Ref. [5].

Table 1
Sulfide materials for cathode applications [13].

	CAS-No.	m_r/g·mol^{-1}	ρ/g·cm^{-3}	mp/°C	dp/°C	κ (25 °C)/Ω^{-1}·cm^{-1}	κ (400 °C)/a.u.
FeS_2	1317-66-4	119.967	5.2	1171	450	0.575	Semiconductor
CoS_2	12013-10-4	123.06	4.80	–	650	5,000.0	Metallic
NiS_2	12035-51-7	122.8	4.45	1007	550	1.667	Semiconductor

Similarly, as for the anode the cathode is not pure sulfide material but contains electrolyte and porous MgO as both binder and wetting agent to improve interaction between the electrolyte and the cathode.

Another material investigated for thermal batteries is NiS_2 which possesses an intermediate decomposition temperature but similar to FeS_2 is a semiconductor too at high temperatures [14]. Table 1 displays important properties of sulfides used as cathode materials.

1.3. Electrolytes

Typical electrolytes used in molten salt batteries are binary and ternary eutectics from alkali halide salts such as LiCl-KCl (mp: 352 °C) or LiF-LiCl-LiBr (mp: 445 °C) [15]. With the binary electrolyte precipitation of $LiK_6Fe_{24}S_{26}Cl$ phase due to reaction of iron(IV) sulfide with potassium chloride melt has been observed [16]. For mechanical stabilization of the molten electrolyte against spin, and acceleration forces (upon function) it is blended with a binder such as porous MgO that contains the molten electrolyte by capillary forces. Typically, electrolytes comprise between 30 wt% – 35 wt% MgO as binder [11]. Table 2 shows the conductivity, κ, of various molten salts in comparison with aqueous ionic solutions.

The composition of typical thermal batteries and their performance characteristics are given in Table 3.

Table 2
Electrical Conductivities of various ionic liquids [5,8,11,17,18].

Ionic liquid/mol%	mp/°C	κ/Ω^{-1} cm^{-1}
LiCl	610	5.83 (at 620 °C)
NaCl	801	4.17 (at 1000 °C
KCl	770	2.24 (at 800 °C)
KI	681	1.30 (at 700 °C)
LiCl-KCl (58.8/41.2)	354	1.69 (at 475 °C)
LiCl-LiI (63/65)	368	3.88 (at 475 °C)
LiF-LiCl-LiBr (21/23/56)	443	3.21 (at 475 °C)
LiF-LiCl-LiBr-NaCl (15/13/62/10)	430	3.16 (at 500 °C)
LiF-LiCl-LiBr-NaBr (15/22/53/10)	430	3.17 (at 500 °C)
LiF-LiBr-LiI (13/34/53)	375	3.18 (at 500 °C)
CaF_2	1423	3.56 (at 1550 °C)
*NaCl solution (*1 mol/l *H_2O)*	n.a.	0.074 (at 20 °C)
Saturated NaCl solution (~5 mol/l *H_2O)*	n.a.	0.214 (at 20 °C)
*LiCl solution (*1 mol/l *H_2O)*	n.a.	0.063 (at 20 °C)

1.4. Thermal activation & discharge

The first thermal battery was invented by German Georg Otto Erb in the 1940s and found mass use as a fuse battery in the A4 ballistic missile. This battery - based on calcium/calcium chromate – did not require a pyrotechnic heating charge but harvested the excess thermal energy provided by the rocket engine [19]. Similarly, thermally activated cells bearing no pyrotechnics are in continuous use in borehole applications where high temperatures are encountered. Apart from these applications the use of thermal batteries in most missiles and projectiles requires an autonomous heat source that can be triggered.

To activate thermal batteries pyrotechnic heating pellets are required which are integrated regularly in the stack of cells as is depicted in Fig. 1. Upon ignition the heat released causes the electrolyte to liquefy and the battery starts operating.

In order to function in the desired way these pyrotechnics have to satisfy a number of requirements, these are:

- No or at least very little permanent gaseous products formation upon combustion to avoid pressurization of the cell.
- Upon combustion the composition must maintain its physical shape and should not melt at any stage.
- The reacted compacted pellet must be a good electrical conductor.
- The reaction should not release excessive heat to avoid destruction of either anode or cathode.
- The reaction should initiate and proceed very rapidly.
- The reaction products should not cause any detrimental reaction with either anode or cathode.

Reviews on thermal batteries and on various pyrotechnics, have been written by Sheptunov [20] Almada et al. [21], Mosier-Boss et al. [22] and Guidotti & Masset [3,7,10,12,15].

2. Pyrotechnic compositions

2.1. Igniter composition – zirconium/barium chromate - pyrolant and heat paper

A pyrotechnic system originally used as pyrotechnic pellet in thermal batteries is the so-called “Heat paper”. Heat paper is a glass-fibre substrate impregnated with a pyrolant based on Zr/

Table 3
Typical materials used in thermal battery systems [5,8,11].

System			
Anode	Calcium	LiX	LiSi
Electrolyte	LiCl-KCl	LiCl-KCl	LiCl-KCl-LiBr
Cathode	$CaCrO_4$	FeS_2	CoS_2
Voltage/V	2.60–2.20	X = Al: 1.8, S=Si: 1.95	1.7
Power Density/mA·cm^{-2}	100–800	100–1500	
Theoretical Specific Energy/Wh·kg^{-1}	540	1380	
Practical specific Energy/Wh·kg^{-1}	5–15	50–80	110
Temperature range/°C	400–550	350–400	up to 650
Discharge time/min	up to 5	up to 60	up to 120
Drawbacks	$CaLi_2$- formation	$LiK_6Fe_{24}S_{26}Cl$ formation	High price of CoS_2

$BaCrO_4$ and an inorganic silicate binder [23]. For impregnation the glass fiber mat (which is of a thickness in the order of 0.30–0.35 mm) is guided through an applicator that is filled with an aqueous slurry containing the pyrolant mix $Zr/BaCrO_4$ and alkaline aluminium silicate, $(AlO)_2SiO_3$ the latter which serves as binder. After wiping off surplus pyrolant slurry the impregnated tape enters a thermal dryer and is wound up. The heat paper pyrolant composition typically ranges around 20 ± 2 wt% zirconium. The calorific content is ~1740 ± 20 $J \cdot g^{-1}$ with a burn rate of ~160 mm s^{-1}.

Modifications of this material have become known as Z-2 or Z-3. A composition using ZrNi alloy instead of Zr is termed T-2 [24]. Heat paper based on $Zr/BaCrO_4$ is sensitive to impact and extremely sensitive to electrostatic discharge which makes handling of this highly dangerous. On top chromium(VI) compounds are objectionable components and as such formulations based on them have to be replaced. The calorific output of $Zr/BaCrO_4$ heat paper upon ageing through hot storage drops significantly when exposed to temperature equal and excess of 150 °C. Similarly, the burn rate of heat paper drops for the same conditions [25]. Heat paper is still in use as a pyrotechnic first fire in some battery designs, however, given its high content in objectionable barium chromate(VI) replacements are sought for the latter which could include molybdates [26] or tungstates [27] of alkaline earth metals.

2.1.1. Thermochemistry of $Zr/BaCrO_4$

The enthalpy of explosion for a series of binary $Zr/BaCrO_4$ pyrolants has been determined experimentally by Ellern and is reproduced below in Table 4 both per unit mass and unit volume [24]. Those values are compared in Fig. 4 with the calculated adiabatic combustion temperature indicating that the equilibria established with thermochemical codes do not quite describe the actual chemistry.

The $Zr/BaCrO_4$ (22/78) pyrolant is not very sensitive to thermal stimuli and has a very high differential thermal analysis (DTA) onset temperature of ~896K (623 °C) at 40K min heating rate under argon flow (150 ml min^{-1}) (Fig. 6) [29]. However, the electrostatic discharge 50% initiation energy for a $Zr/BaCrO_4$ (20/80) based on 8.4 μm Zr particles and 0.4 μm barium chromate is only 100 μJ and thus is highly sensitive to electrostatic stimuli [30]. The electrostatic sensitivity for coated Zr pyrolant is much higher than for a pyrolant that bears a coating on the barium chromate only. The burn rate of $Zr/BaCrO_4$ pyrolant with Viton and without has been investigated by Berger [31] and Kuwahara et al. [32]. The binary system exhibits its highest burn rate at $\xi(Zr) \sim 57$ wt%. The pyrolant containing 1 wt% Viton show a maximum burn rate, $u = 22$ mm s^{-1}, at $\xi(Zr) = 40$ wt%. At high Viton content (10 wt%) the burn rate further drops significantly and has a maximum at around 55 wt% Zr ($u = 9$ mm s^{-1}(see Fig. 5).

Table 4
Enthalpy of Combustion of binary $Zr/BaCrO_4$ mixtures, after Ref. [24].

Zr/wt%	15	20	25	30	35	40	45	50
$\Delta_{ex}H/kJ \cdot g^{-1}$	1255	1619	1828	1966	2050	2113	2029	1904
$\Delta_{ex}H/kJ \cdot cm^{-3}$	5917	7758	8906	9740	10330	10834	10589	10117

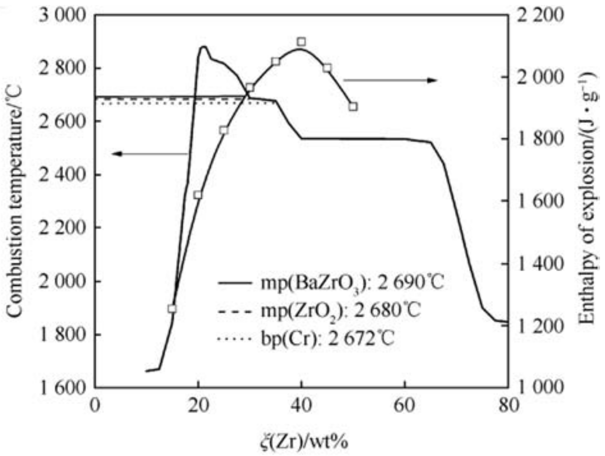

Fig. 4. Calculated adiabatic combustion temperature with EKVI [28] and experimental enthalpy of explosion [24] of $Zr/BaCrO_4$ as function of stoichiometry.

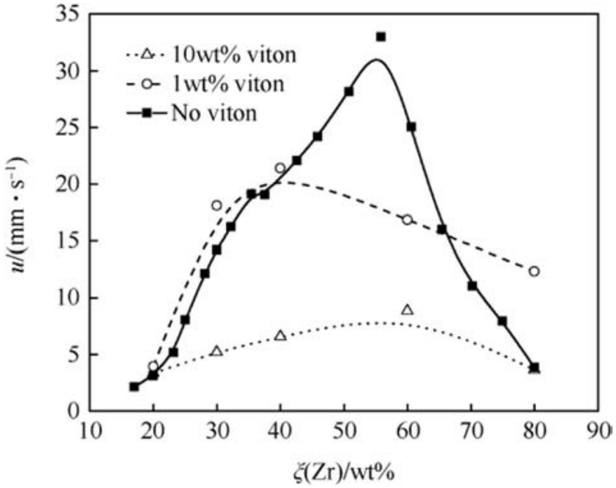

Fig. 5. Burn rate of $Zr/BaCrO_4$ and $Zr/BaCrO_4$/Viton after Ref. [31,32].

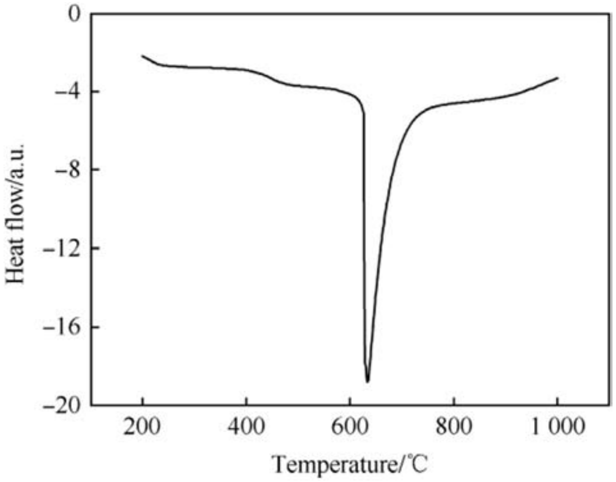

Fig. 6. DTA of $Zr/BaCrO_4$ (20/80) under Argon and at 40 K min^{-1} heating rate, after ref. [29].

Separately coating Zr, $BaCrO_4$ or both components with 1 wt% Viton binder reveals that coating of Zr with Viton enhances the combustion rate whereas coating the barium chromate slows down the burn rate. However, these effects become indistinguishable at mass fractions >10 wt% Viton. Lead-tube burn rates for $Zr/BaCrO_4$ with 2 wt% nitrocellulose binder have been determined in Ref. [33].

The DTA of $Zr/BaCrO_4$ exhibits a very high onset temperature of 623 °C, however the presence of Viton lowers the thermal onset. Although determined at lower heating rate (20 °C· min^{-1}) and at

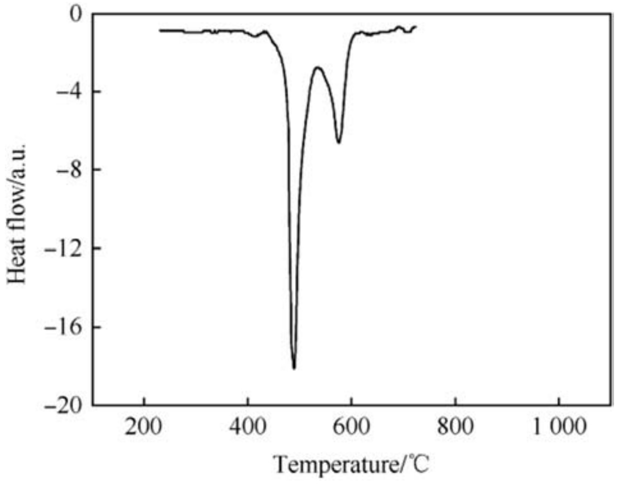

Fig. 7. DSC of Zr/$BaCrO_4$/Viton (57/38/5) under Argon at 20K·min^{-1} heating rate after Ref. [30].

higher ξ(Zr) the onset shifts down by ~ 170 °C–452 °C as is depicted in Fig. 7.

Other than in thermal batteries "Heat paper" has been used as first fire in decoy flares [34].

2.2. Pyrotechnic heater – iron/potassium perchlorate (IPP) - "Heat" pellets

In the early 1960s United States Department of Energy (DOE) and Department of Defense (DOD) sought a replacement for the highly sensitive "Heat paper". Contracts were put out and it was found that fuel rich pyrolants based on spongy iron powder and very fine potassium perchlorate (15 μm) fulfil the above-mentioned requirements. A very detailed history of the development of Fe/$KClO_4$ is given by Guidotti in Ref. [25].

Although the use of iron powder in pyrotechnics may be counterintuitive as we are familiar with the quick oxidation (rusting) of unprotected iron powder at ambient humidity, handling of fine iron powder at reduced humidity (≤3% RH at 20 °C) is technically feasible.

2.2.1. Thermochemistry

The enthalpy of reaction of Fe/$KClO_4$ as function of the stoichiometry in the range between 80 wt% – 90 wt% Fe correlates linearly with the iron content and is given in Table 5. The experimental data have been obtained with NX-1000 iron powder which is described further down below.

Eq. (6) depicts the idealized combustion reaction of a typical pyrolant used in standard thermal batteries having a weight ratio of 88/12 iron/potassium perchlorate.

$$1.576\ Fe_{(s)} + 0.087\ KClO_{4(s)} \longrightarrow 0.348\ FeO_{(s)} + 1.228\ Fe_{(c)} + 0.087\ KCl_{(l)} \qquad (6)$$

The calculated equilibrium combustion temperature of this composition equals 1409K at 0.1 MPa which is still below the vaporization temperature of KCl.

Table 5
Enthalpy of reaction of binary Fe/$KClO_4$ mixtures, after Ref. [35,36].

Iron content/wt%	80	82	84	86	88	90
Exp/J·g^{-1}	1559	1423	1244	1084	928	766
Theor./J·g^{-1}	1582			1107	949	

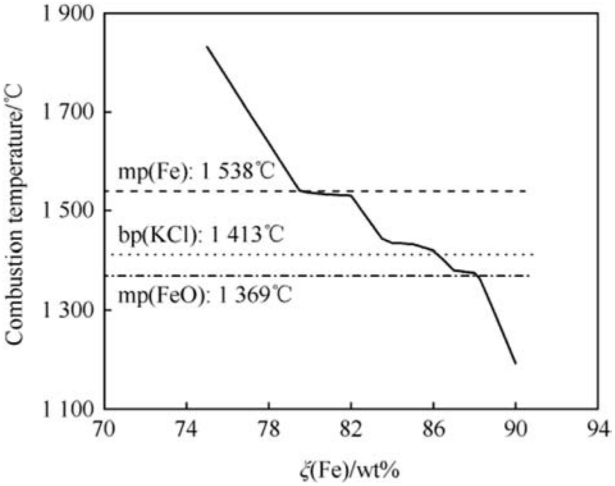

Fig. 8. Adiabatic Combustion temperature of Fe/$KClO_4$ calculated with EKVI [28].

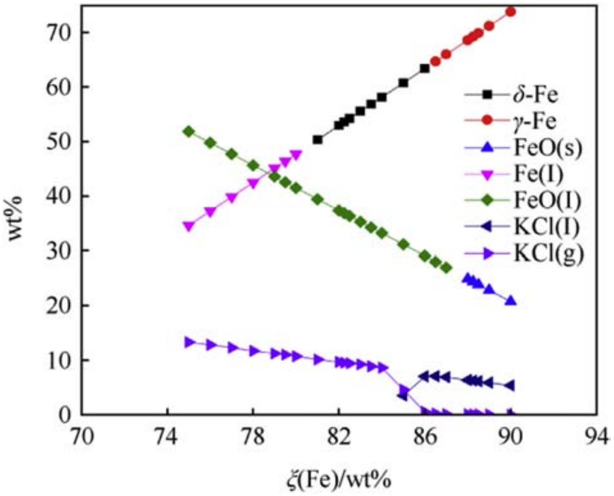

Fig. 9. Equilibrium composition of Fe/$KClO_4$ calculated with EKVI [28].

Fig. 8 shows the adiabatic combustion temperature of Fe/$KClO_4$ for ξ(Fe) ranging between 75 wt% – 90 wt% superimposed on the fusion points of both Fe, FeO and the boiling point of KCl limiting the temperature and thereby causing the local flattening of the curve at the corresponding temperatures. The calculated equilibrium composition at T_c is depicted in Fig. 9 whereas Fig. 10 depicts the calculated composition of the combustion products at ambient temperature.

While calculations predict Fe and Fe_3O_4 to be main combustion product [28] experimental analysis with transmission electron micrography and energy dispersive X-ray analysis (EDX) reveals that unreacted iron particles are covered with a thin (d ~ 200 nm) FeO-shell [37].

As a thermal battery must withstand rough environmental conditions such as shock, impact, spin and extreme acceleration, heat pellets must not disintegrate upon these stimuli. Hence high mechanical strength is required. To achieve this high mechanical integrity Heat pellet-composition requires a sponge-type iron powder which allows for a good interlocking of the granules. Fig. 11 depicts electron micrographs of increasing resolution (left to right) of a sponge type iron designated NX-1000 manufactured by Ametek. The images show the particular branching of the particles

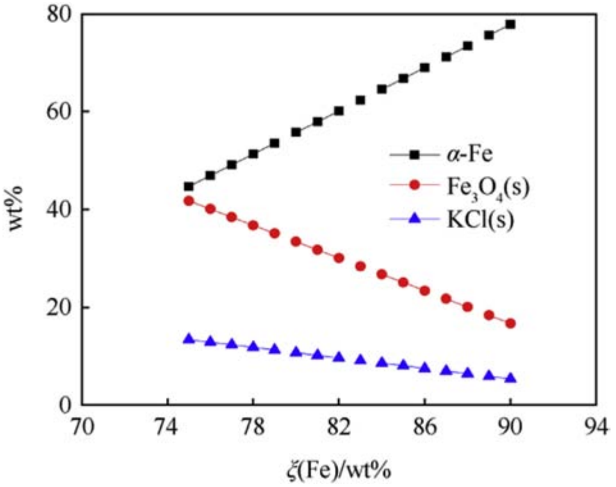

Fig. 10. Ambient temperature composition of Fe/KClO$_4$ combustion products calculated with EKVI [28].

Table 6
Properties of NX-1000 iron powder after Ref. [38].

Sample Type	NX-1000
Total Iron content/wt%	≥97
Metallic Iron content/wt%	≥87
Weight loss on H_2 reduction/%	≤2.3
Green strength/MPa	≥31
Apparent density/g·cm^{-3}	1.5–1.7
−140 mesh	87.6
−80 mesh	8.9
->80 mesh	3.5
Surface Area/m^2·g^{-1}	0.76

which explains for the outstanding mechanical properties of pellets based on this material. The properties of NX-1000 are given in Table 6.

A process for producing iron powders with suitable morphologies for use in heat pellets has been disclosed in Ref. [38].

Heat pellets are typically consolidated to densities higher than 2.75 g cm^{-3} as mechanical strength at lower densities is insufficient. The influence of pellet density on breaking strength of 2.5g test pellets is given in Table 7. The density pressing pressure relationship for two pyrolants is depicted in Fig. 12.

The particle size of the potassium perchlorate used in heat powders affects both burn rate and ignitability of the pellets. Fig. 13 shows the evolution of both parameters. The burn rate increases with increasing KClO$_4$-particle size which is a characteristic for many metal/oxidizer pyrolant systems where the metal melting temperature is well above the decomposition temperature of the oxidizer. The ignition energy surprisingly increases in the same range with increasing particle size as well. The burn rate of Fe/KClO$_4$ is determined in a set-up that mimics the configuration in the final battery and is shown in Fig. 14.

As is evident from Fig. 15 the burn rate decreases as the theoretical density is approached and pellets having densities higher than 4–5g·cm^{-3} cannot be properly ignited and do not sustain combustion.

Thus, it appears that some porosity is required to allow for both ignition and propagation of combustion.

The influence of density on the burn rate of various Fe/KClO$_4$ pyrolant pellets as 31.75 mm diameter pellets has been investigated by Guidotti [36,40]. At ξ(Fe) = 80 wt% a maximum burn rate of $u = 550$ mm s^{-1} is obtained at low density (55% TMD), whereas consolidation of the same pyrolant composition to 80% TMD yields a reduction of the burn rate by more than 50% ($u = 202$ mm s^{-1}). For the pyrolants containing 82 wt% and more iron the influence of density is less pronounced as is depicted in Fig. 16.

Lead tube burn rates of various Fe/KClO$_4$ mixtures using different iron powders have been investigated by Callaway et al. [41]. Fig. 17 shows the burn rate as function of the stoichiometry for three different iron powders whose characteristics are compared in Table 8.

Heat pyrolant stemmed into lead tubes yields much lower burn rates as those consolidated to pellets. Obviously, the lead tubing ($\lambda_{Pb} = 35$W/(m· K)) effects dissipation of heat and slows down the burn rate. A pyrolant using a multimodal spherical iron powder (see Fig. 18) yields burn rates in excess of 50% of those based on NX-1000.

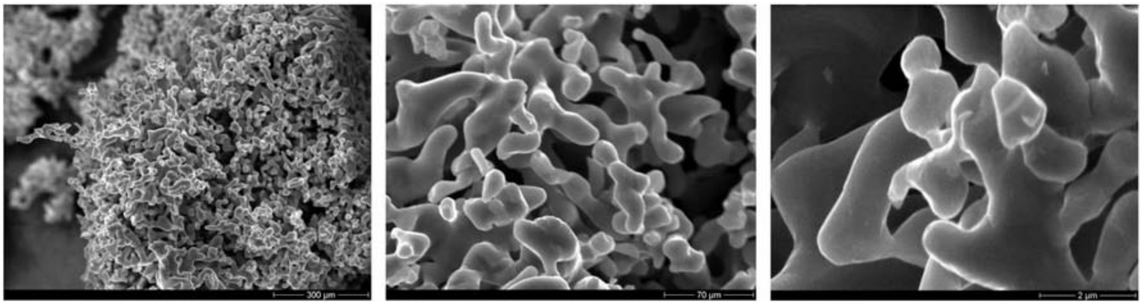

Fig. 11. Electron micrographs of NX-1000 sponge iron manufactured by Ametek.

Table 7
Effect of pellet density on breaking strength for (88/12 Fe/KClO$_4$) from Ref. [35].

Pellet Density/g·cm^{-3}	Consolidation Pressure/MPa	Average Breaking Strength/N	50%-Ignition Energy/J
3.30	73.08	1.15	0.182
3.40	87.56	1.38	0.164
3.50	96.53	1.73	0.161
3.60	112.38	1.91	0.248
3.70	135.14	2.09	0.253

The combustion rate of Heat pellets increases with temperature but does not vary with thickness of the pellet.

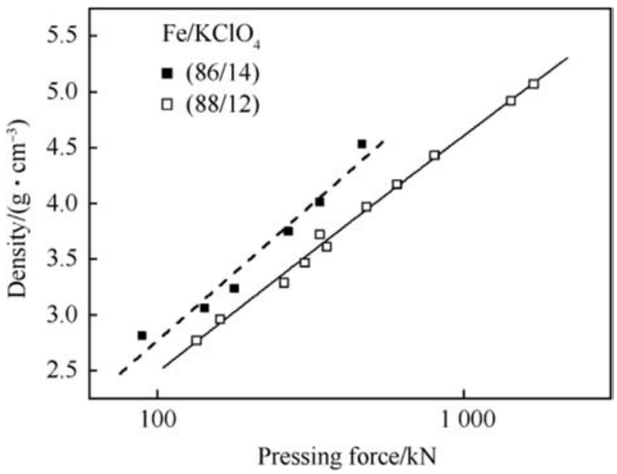

Fig. 12. Effect of consolidation Force on density after Ref. [39].

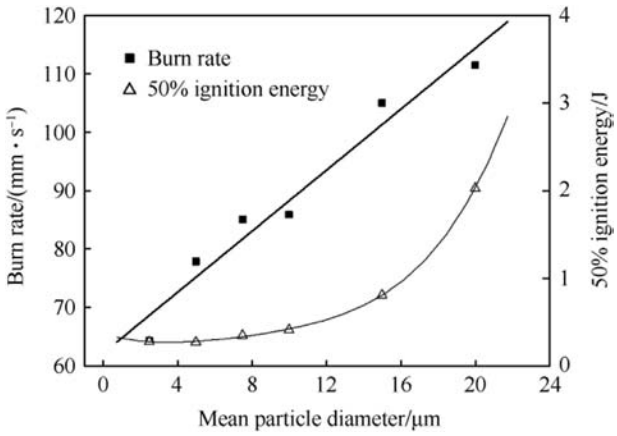

Fig. 13. Effect of $KClO_4$ particle size of burn rate and ignition energy for 88/12 IPP after Ref. [35].

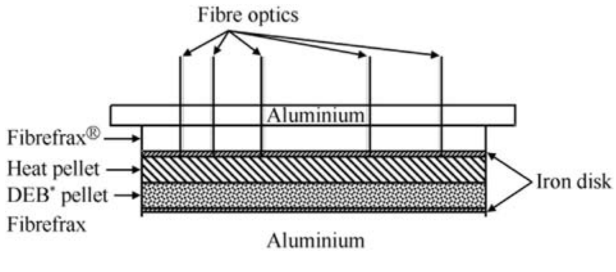

Fig. 14. Burn rate measurement setup. *DEB = Depolarizer($CaCrO_4$), Electrolyte (LiCl-KCl), Binder (SiO_2).

The burn rate of Heat (84/16) prepared from a Fe powder obtained by spray pyrolysis at different temperatures increases with the pyrolysis temperature as is indicated in Table 9 [42].

2.2.2. Thermal studies & stability

Callaway et al. studied the reaction of (80/20) Heat powder in the DSC under air at 10 K min^{-1} heating rate. Fig. 19 show DSC-traces for both powdered and pelletized material. The pelletized material shows a distinct pre-ignition reaction directly after the

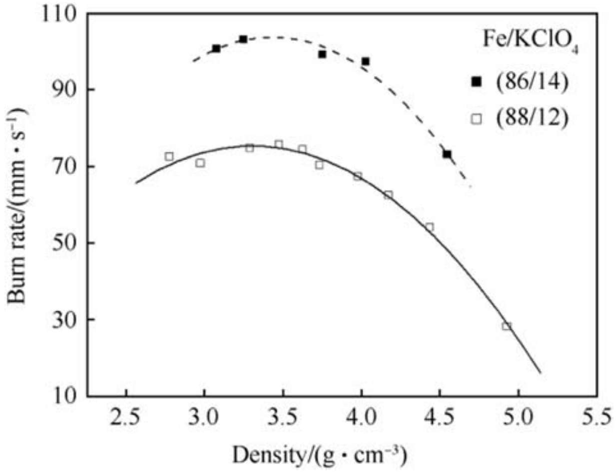

Fig. 15. Influence of density on Burn rate of Two Heat pyrolants after Ref. [19].

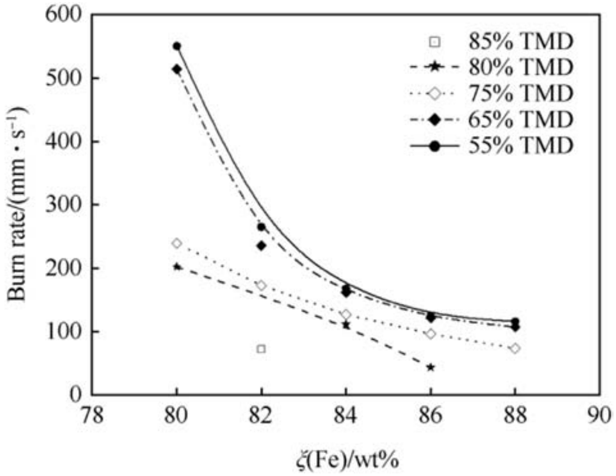

Fig. 16. Influence of density on Burn rate of Heat pyrolants after Ref. [36,40].

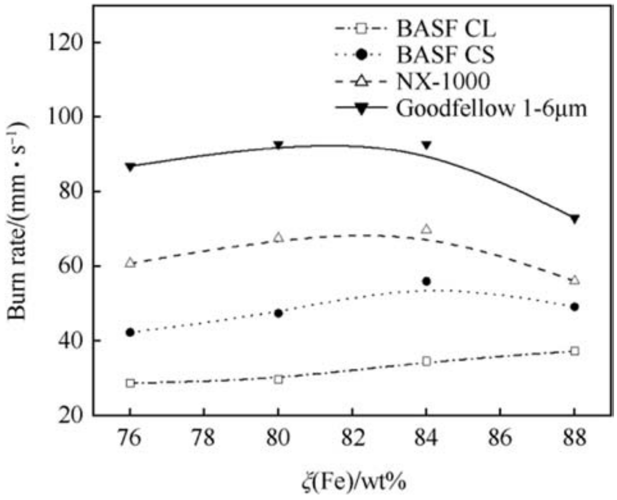

Fig. 17. Lead tube burn rate measurement of Heat powders based on various iron qualities after Ref. [41].

Table 8
Properties of iron powders studied in Ref. [41].

Material	Specific Surface Area/$m^2 \cdot cm^{-3}$	Mean Surface Diameter/μm
NX 1000	0.248	1.5–3.5
BASF CS	0.974	4–5
BASF CL	0.729	7–8
Goodfellow 1–6 μm	2.31	1–6

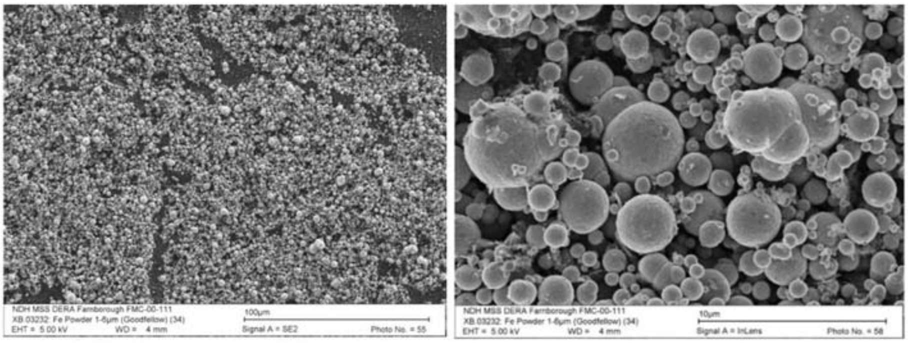

Fig. 18. Electron micrographs of Goodfellow iron powder as quoted by Callaway et al. courtesy of International Pyrotechnics Society [41].

Table 9
Burn rate of consolidated Heat 84/16 as function of pyrolysis temperature [42].

Preparation temperature/°C	Burn rate/$mm \cdot s^{-1}$
700	65
900	82
1000	86

Table 10
Kinetic parameters for ($Fe/KClO_4$) Heat powder [43].

ξ(Fe)/wt%	82	84	86	88
$E_A/kJ \cdot mol^{-1}$	215	217	223	228
ln A	29.01	29.16	30	29.77

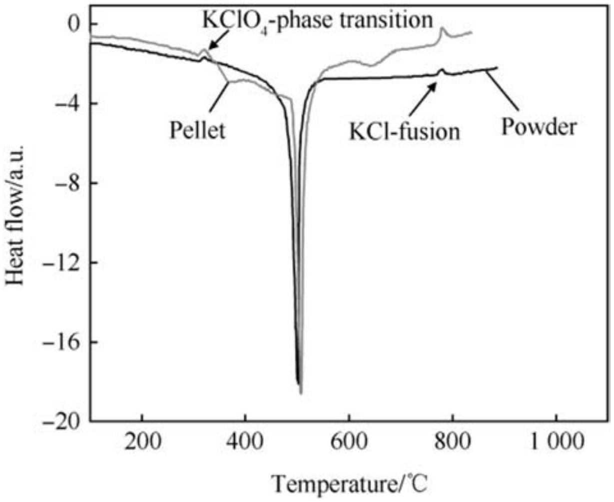

Fig. 19. DSC studies of $Fe/KClO_4$ (80/20) by Callaway et al. after Ref. [41].

$KClO_4$-phase-transition at 299 °C and a steep onset of the main oxidation reaction at 480 °C. At 772 °C the melt endotherm for potassium chloride is observed.

Kinetic data for Heat pellets (Fe: 44 μm, 99.9%; $KClO_4$: 10 μm, 99.9%) has been determined by Alkan et al. [43]. Table 10 shows the activation energy and preexponential factor for a range of formulations which is about in the same ballpark and which also reflects the observation by Reinholz et al. [44] that ignition energy of Heat does not vary appreciably with stoichiometry in the considered range.

Exposure of $Fe/KClO_4$ (88/12) heat pellets to humidity levels equal and greater than 33% RH affects calorific output, ignition energy and burn rate as is depicted in Table 11. Also, hot storage under dry conditions affects burn rate and ignitability [25].

23% RH does neither affect calorific output nor ignitability. However, exposure to 33% RH and humidity above yield both reduction in calorific output and frequent ignition failures [25,44]. The ignition of Heat pellets in an Argon filled shock tube has been investigated by Evans [45]. Gillard et al. studied the Laser-ignition of Heat pellets [46]. Koyuncu et al. have developed

Table 11
Influence of storage conditions on ignition and calorific output.

Environment	Exposure time	Effect on Ignition Energy	Ignition failures	Effect on Burn rate	Effect on Calorific Output
23% RH	30 days	No effect	n.t.	No effect	n.t.
23% RH	6 months	Possible incr.	none	No effect	No change
33% RH	2 days	50% incr.	n.t.	30% decr.	n.t.
33% RH	7 days	50% incr.	none	50% decr.	6.2% decr.
42% RH	16 h	88% incr.	some fail.	42% decr	4.5% decr.
42% RH	2 days	667% incr.	14/25	83% decr.	12.4% decr.
52% RH	4 h	27% incr.	none	14% decr.	1.6% decr.
52% RH	1 day	114% incr.	3/5	47% decr.	5.1% decr.
50 °C dry	37 months	29.4% incr.	n.t.	8.5% incr.	n.t.
75 °C dry	37 months	59% incr.	n.t.	3.2% decr.	n.t.

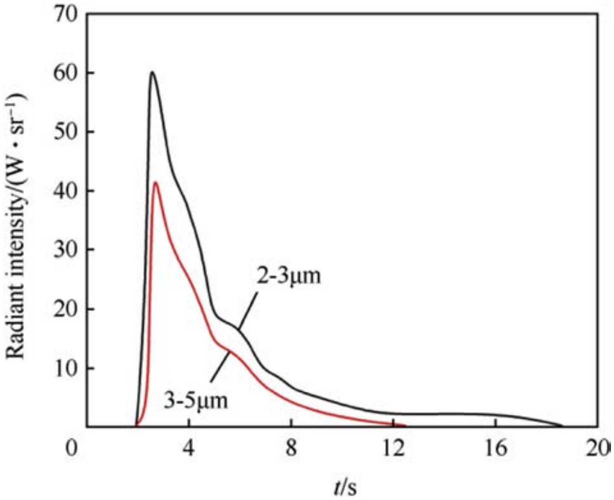

Fig. 20. Radiometric profile of single 60 mm diameter Heat (86/14) pellet in still air at ambient pressure.

a model to describe the combustion of Heat pellets and the temperature evolution of thermal battery stacks comprising them [47].

Heat powders containing other iron powder qualities than NX-1000 have been investigated in great detail by Czajka & Wachowski et al. [48–52]. The same authors also studied the effect of catalytic amounts of iron oxides present on the surface of iron powder on the decomposition of KClO$_4$ [53].

2.2.3. Other uses

Heat Pellets have been proposed as blackbody emitters for use in infrared decoy flares by Callaway [54]. Fig. 20 shows the radiometric profile for a 60 mm diameter disc in 2–3 μm and 3-5 μm-band. Unlike typical pyrotechnic flares the combustion of those pellets yields very little smoke (mainly infrared-transparent KCl$_{(s)}$) which effects unobscured emission of infrared radiation.

3. Hazards

As thermal batteries contain both energetic (Heat) and combustible materials (Li-alloys) they are often classified under Hazard Division HD1.4S [55]. The general hazards encountered with thermal batteries are the high container temperatures encountered upon firing and the resulting danger of fire for flammable materials adjacent to it. The hazards of bulk amounts of heat powder (84/16) have been investigated by Guidotti et al. [56]. Unexpected ignition of large bulk (3.6 kg) heat powder produces large fires which can have disastrous outcome. The loose material shows rapid ignition (<100 ms) and yields temperatures in excess of 1200 °C. The issues relating to the disposal of thermal batteries have been addressed in Refs. [57,58] respectively.

No information is available in the public domain on the response of thermal batteries to Insensitive Munitions Test [59].

4. Outlook

Leventis et al. [60] have prepared iron(0) aerogels infiltrated with KClO$_4$ which show an inherent high degree of porosity and exhibit extreme high combustion rate. Replacement of perchlorates is considered in some countries a necessary step and hence other alternative halogen-free oxidizers are sought. Potential candidates include transition metallates [26,27] including potassium ferrate(VI) K$_2$[FeO$_4$] the latter which has been investigated in detail by Pliskin et al. [61,62]. *Poret* et al. have proposed to use Ni/Al multireactive layers commercially known as Nanofoil® to heat thermal batteries [63] likewise other intermetallic systems have been considered as potential replacement for Heat [64].

5. Summary

State of the art thermally activated batteries use an alkali halide eutectic mixture that serves as electrolyte. The anode of thermal batteries is based on high melting alloys of lithium, the cathode uses either iron disulfide or cobalt disulfide which in comparison to the former allows for higher operating temperatures. To trigger a thermal battery a stack of pyrotechnic heating pellets is ignited that upon combustion develops sufficient heat to liquify the electrolyte. Those heating pellets are commonly composed from a dendritic iron powder and potassium perchlorate with iron contents in the 84 wt%-86 wt% ballpark.

Acknowledgement

The author thanks the referees for pointing out errors and inconsistencies and for sharing valuable information on cathode reaction.

References

[1] Koch E-C. Special materials in pyrotechnics: V. Military applications of phosphorus and its compounds. Propellants Explos Pyrotech 2008;33:165–76.
[2] Koch E-C, Clement D. Special materials in pyrotechnics: VI. Silicon - an old fuel with new perspectives. Propellants, Explos Pyrotech 2007;32:205–12.
[3] Guidotti RA, Masset P. Thermally activated ("thermal") battery technology Part I: an overview. J Power Sources 2006;161:1443–9.
[4] Dekel DR, Taubenfeld Z, Melchior S. Thermal battery activation by direct ignition of pyrotechnic pellets. Fort Collins, CO, USA: 31st International Pyrotechnics Seminar; 2004. p. 137–44.
[5] Ritchie AG. Molten salt electrolytes in high temperature batteries, M&S 1155. Farnborough, UK: Royal Aerospace Establishment; 1990.
[6] Dallek S, Ernst DW, Larrick BF. Lithium –boron alloy anodes for molten salt batteries, NSWC/WOL TR 77-67. Dahlgren, VA, USA: Naval Surface Warfare Center; 1977.
[7] Guidotti RA, Masset PJ. Thermally activated ("thermal") battery technology: Part IV: anode materials. Power Sources 2008;183:388–98.
[8] Krieger FC. Thermal battery systems for ordnance fuzing, DL-TR-1089. Adelphi, USA, H: US Army Electronics Research and Development Command, Harry Diamond Laboratories; 1982.
[9] Masset P. Thermal stability of FeS$_2$ cathode material in "thermal" batteries: effect of dissolved oxides in molten salt electrolytes. Z Naturforsch 2008;63a: 596–602.
[10] Masset PJ, Guidotti RA. Thermally activated ("thermal") battery technology: Part IIIa: FeS$_2$ cathode material. Power Sources 2007;177:595–609.
[11] Guidotti RA, Reinhardt FW. Evaluation of the Li(Si)/FeS$_2$ and Li(Si)/CoS$_2$ couples for a high-voltage, high-power thermal battery, SAND2000-1408. Albuquerque, NM, USA: Sandia National Laboratories; 2000.
[12] Masset PJ, Guidotti RA. Thermally activated ("thermal") battery technology: Part IIIb: sulfur and oxide-based cathode materials. Power Sources 2007;178: 456–66.
[13] Pearce CI, Pattrick RAD, Vaughan DJ. Electrical and magnetic properties of sulfides. Rev Mineral Geochem 2006;61:127–80.
[14] Payne JL, Percival JD, Giagloglou K, Crouch CJ, Carins GM, Smith RI, Comrie R, Gover RKB, Irvine JTS. In-situ thermal battery discharge using NiS$_2$ as a cathode material. ChemElectroChem 2017;4:1916–23.
[15] Masset PJ, Guidotti RA. Thermal activated (thermal) battery technology: Part II: molten salt electrolytes. Power Sources 2007;164:397–414.
[16] Melendres CA, Sy CC, Tani B. Anodic sulfidation of iron in molten LiCl - KCl. J Electrochem Soc 1977;124:1060–3.
[17] Lore JD. Electrical conductivity measurements of molten-salt fluxes from an electroslag remelting process, report Y-1947, Oak ridge Y-12 plant, TN, USA. 1974. p. 19.
[18] Van Artsdalen ER, Yaffe IS. Electrical conductance and density of molten-salt-systems, KCl-LiCl, KCl-NaCl, KCl-KI. J Phys Chem 1955;59:118–27.
[19] Guidotti RA, Preston S. Electrode fabrication processes for thermal batteries, AIAA 2007-4706. In: 5th international energy conversion engineering conference, Str Louis, MS, USA; 2007.
[20] Sheptunopv VN. Heat generating compositions for thermal batteries. Elektrotekh Prom St Khim Fiz Istochniki Toka 1983;5:16–9.

[21] Almada GF, Vieira MJP, Rupp MTC, Ponzio EA. Baterias termicas: revisao. Rev Virtual Quim 2013;5:563–95.

[22] Mosier-Boss PA, Szpak S. Electrochemical systems with high power density. An overview, technical document 1715. San Diego, CA, USA: Naval Ocean Systems Center; 1989.

[23] Fischbach, A., Teti, J. E. (1974), Improvements in or relating to thermal batteries (filed 4 March 1957), GB Patent 1 346 565, USA.

[24] Ellern H. Military and civilian pyrotechnics. New York: Chemical Publishing Company; 1968. p. 282–3.

[25] Guidotti R. Development history of Fe/KClO$_4$ heat powders at sandia and related aging issues for thermal batteries, SAND2001-2191. Albuquerque, NM, USA: Sandia National Laboratories; 2001.

[26] Sabatini JJ. Green pyrotechnics. In: Brinck T, editor. Green energetic materials. New York: John Wiley; 2013. p. 63–101.

[27] Jolicoeur, B., Palardy, M. (2018), Tungsten Oxide Primer Composition, US Patent Appl. 20180258007A1, USA.

[28] Noläng B. EKVI-code, version 4.6.1. Uppsalla, Sweden: BeN-Systems; 2016.

[29] Czajka B, Styczynski S, Tabat S, Szal D. Determination of ignition sensitivity of selected heat powders. Centr Eur J Energ Mater 2011;8:3–13.

[30] Kuwahara T, Kohno T, Wang CH. Static electric sensitivity characteristics of Zr/BaCrO$_4$ pyrolants. Propellants, Explos Pyrotech 2004;29:56–61.

[31] Berger B. Bestimmung der Abbrandcharakteristik sowie der Sicherheitskenndaten verschiedener binaerer pyrotechnischer Anzünd- und Verzögerungssysteme. In: Annual ICT conference, Karlsruhe, V-72; 1986.

[32] Kuwahara T, Kohno T, Wang CH. Coating effect to burning rate and sensitivity characteristics of Zr/BaCrO$_4$ pyrolants, AIAA 2002-3747. In: 38th AIAA/ASME/SAE/ASEE joint propulsion conference & exhibit, 7-10 July 2002, Indianapolis, IN, USA; 2002.

[33] Daniel R, Sarawadekar RG. Pyrotechnic compositions of zirconium and chromates of alkaline earth metals. In: International annual conference of ICT, Karlsruhe, Germany, V-48; 1995.

[34] Douda BE. *Genesis of infrared decoy flares – The early years from 1950 into the 1970s*, NSWCCR/RDTR-08/63. IN, USA: NSWC-Crane, Crane; 2009. p. 184.

[35] Rittenhouse CT. Final report on the development of pelletized heat sources for thermal batteries, *SC-CR-70-6137*. AZ, USA: Unidynamics Phoenix, Inc; 1970.

[36] Guidotti RA, Odinek J, Reinhardt FW. Characterization of Fe/KClO4 heat powders for thermal batteries. In: 29th international pyrotechnics seminar, July Westminster, CO, USA; 2002. p. 847.

[37] Chong J, Xun S, Battaglia VS. Insight into iron heat-powder combustion products for thermal batteries: core-shell structure and semiconductive properties. Electrochem *Solid-State Lett* 2011;14:A123–5.

[38] Welbon, W.W. (1983), Process for the Synthesis of Iron Powder, US Patent 4 414 021, USA.

[39] McCarthy DK, Leslie WB, Dietzel RW. Burn front velocity as A function of pellet density in iron/potassium perchlorate heat powders, SAND83-1025. Albuquerque, NM, USA: Sandia National Laboratories; 1985.

[40] Guidotti RA, Odinek J, Reinhardt FW. Characterization of Fe/KClO$_4$ heat powders and pellets. J Energ Mater 2006;24:271–305.

[41] Callaway J, Davies N, Stringer M. Pyrotechnic heater compositions for use in thermal batteries. Adelaide, Australia: International Pyrotechnics Seminar; 2001. p. 153.

[42] Kim JH, Koo HY, Hong SK, Han JM, Jang HC, Ko YN, Hong YJ, Kang YC, Kang SH, Cho SB. Combustion characteristics of the heat pellet prepared from the Fe powders obtained by spray pyrolysis. Adv Powd Tech 2012;23:387–92.

[43] Alkan A, Koyuncu T, Can M, Teksen T, Yesilirmak Ünsal E, Göcmez A. Determination of kinetic parameters for Fe/KClO$_4$ pellets used in thermal batteries. In: 48th power sources conference, Denver, CO, June 11-14, 2018; 2018. p. 165–8.

[44] Reinholz EL, Wesolowski DE. Manufacturing and temperature effects on heat pellet ignition sensitivity. Albuquerque, NM. USA: SAND2014-2938C Sandia National Laboratory; 2014. p. 4.

[45] Evans NA. Pyrotechnic ignition studies using a gun tunnel. In: 14th international pyrotechnics seminar, Jersey, UK; 1989. p. 112.

[46] Opdebeck F, Gillard P, Radenac d'E. Influence of interface conditions on laser diode ignition of pyrotechnic mixtures: application to the design of an ignition device. Int J Therm Sci 2003;42:47–56.

[47] Koyuncu T, Alkan A, Sevim K, Yesilirmak Ünsal E, Göcmez A. Modeling of pyrotechnic combustion behavior and temperature distribution for the ignition phase of thermal batteries. In: 48th power sources conference, Denver, CO, June 11-14, 2018; 2018. p. 428–31.

[48] Czajka B, Tabat S, Stycczynski Wachowski L, Zielinski M, Pietrowski M. Physicochemical properties of iron powders used as reducing agents in materials of high calorific value. Cent Eur J Energetic Mater 2004;1:75–88.

[49] Czajka B, Wachowski L. Some thermochemical properties of high-calorific mixture of Fe-KClO$_4$. Cent Eur J Energetic Mater 2005;2:55–68.

[50] Czajka B, Wachowski L. Activator- induced modification of selected properties of heat generating Fe-KClO$_4$ mixture. Cent Eur J Energetic Mater 2006;3:51–63.

[51] Czajka B, Wachowski L, Lapinski A, Rzodkiewicz W. Modification of the surface of the iron powder as an ingredient of the high-calorific mixture. Cent Eur J Energetic Mater 2008;5:87–102.

[52] Czajka B, Wachowski L, Stycczynski S, Tabat S, Szal D. Determination of ignition sensitivity of selected heat powders. Cent Eur J Energetic Mater 2011;8:3–13.

[53] Wachowski L, Czajka B. Textural and catalytic properties of the Fe_xO_y/Fe-KClO$_4$ system. Thermochim Acta 2001;435:102–7.

[54] Callaway J. Expandable infrared radiating means, GB 2387430, United Kingdom. 2003.

[55] N.N. Hazard classification of U.S. Military explosives and munitions, revision 17. McAlester, OK, USA: U.S. Army Defense Ammunition Center, U.S. Army Technical Center for Explosives Safety; 2017. 256 pp.

[56] Nissen M, Guidotti RA, Berry B. Combustion of bulk 84% Fe/16% KClO$_4$ heat powder, report SAND-96-0861C. Albuquerque, NM: Sandia National Laboratories; 1995. 4 pp.

[57] Dow J, Batchelor C. Navy lithium battery safety. In: Department of Defense explosives safety board seminar (34th) held in portland, Oregon on 13-15 July 2010; 2010. 31 pp.

[58] Diem MH. Hazardous waste study, evaluation of thermal batteries for hazardous waste characteristics. , MD, USA: U.S. Army Environmental Hygiene Agency, Aberdeen Proving Ground; 1980. 11 pp.

[59] NATO Standardization Agency. Policy for the introduction and assessment of insensitive munitions (IM), STANAG 4439 JAIS. third ed. 2010 [Brussels, Belgium].

[60] Leventis N, Donthula S, Mandal C, Ding MS, Sotirou-Leventis C. Explosive versus thermite behavior in iron(0) aerogels infiltrated with perchlorates. Chem Matter 2015;27:8126–37.

[61] Wilharm CK, Chin A, Pliskin S. Thermochemical calculations for potassium ferrate(VI), K_2FeO_4, as a green oxidizer in pyrotechnic formulations. Propellants, Explos Pyrotech 2013;39:173–9.

[62] Chin, A., Pliskin, S., Wilharm, C. K. (2015), Ferrate Based Pyrotechnic Formulations, US Patent 020150376079A1, USA.

[63] Prentice, J. L. (1979), Heat Sources for Thermal Batteries: Exothermic Intermetallic Reactions, US Patent 4 158 084.

[64] Poret JC, Ding M, Krieger F, Swank J, Chen G, McMullan C. Nanofoil heating elements for thermal batteries. In: Proceedings of the army science conference (26th) held in Orlando, FL, USA, 1-4 December 2008; 2008. 6 pp.

Abbreviations

$\Delta_{ex}H$: enthalpy of explosion, kJ g^{-1}
κ: conductivity, Ω^{-1} cm^{-1}
$\xi(X)$: Stoichiometric fraction of a substance X, wt.-%
bp: Boiling Point, °C
E_A: Activation energy, kJ
IPP: Iron - Potassium Perchlorate, Fe, KClO$_4$
mp: Melting point, °C
RH: Relative humidity at given temperature, %
u: Burn rate, mm s^{-1}